

Accurate measurement of the cutoff wavelength in a microstructured optical fiber by means of an azimuthal filtering technique

Laurent Labonte, Dominique Pagnoux, and Philippe Roy

Xlim/Photonics Department, UMR CNRS 6172, and University of Limoges, 123 Avenue A. Thomas, 87060 Limoges, France

Faouzi Bahloul and Mourad Zghal

Ecole Nationale d'Ingénieurs de Tunis, BP37, Le Belvédère, Tunis, Tunisia and Sup'Com, 2083 El Ghazala Ariana, Tunisia

Gilles Melin and Ekaterina Burov

Alcatel Research and Innovation, Route de Nozay, 91460 Marcoussis, France

Gilles Renversez

Institut Fresnel, UMR CNRS 6133, and Faculté des Sciences de St Jérôme, University Paul Cézanne Aix-Marseille III, 13397 Marseille, France

Received December 22, 2005; revised March 6, 2006; accepted March 28, 2006; posted March 31, 2006 (Doc. ID 66858)

A simple self-referenced nondestructive method is proposed for measuring the cutoff wavelength of microstructured optical fibers (MOFs). It is based on the analysis of the time-dependent optical power transmitted through a bow-tie slit rotating in the far-field pattern of the fiber under test. As a first demonstration, the cutoff wavelength of a 2 m MOF sample is found to be close to that provided by numerical predictions (~ 25 nm higher). Because of the high dynamics of the measurement, the uncertainty is limited to $\Delta\lambda = \pm 10$ nm. © 2006 Optical Society of America

OCIS codes: 060.2270, 060.2430, 060.2400, 060.2310.

Since their invention 10 years ago microstructured optical fibers (MOFs) have attracted a lot of interest because they offer the possibility of managing the propagation characteristics of guided light in a much larger range than in conventional fibers.¹ In particular, it has been demonstrated that MOFs can be endlessly single mode when the condition $d/\Lambda \sim < 0.4$ is fulfilled, d being the diameter of the holes and Λ being the pitch of the hole lattice.² Otherwise, efficient supercontinuum generation and other nonlinear processes have been achieved in MOFs with a small core surrounded by one or a few rings of large holes, in which the zero dispersion wavelength is shifted toward short wavelengths.³ In such applications, the endlessly single-mode condition is not fulfilled. This means that there is a cutoff wavelength, commonly called λ_c , under which higher-order modes can propagate and the value of which must be precisely determined. The modal cutoff of MOFs has already been theoretically investigated by considering perfect but finite-size structures.⁴ These works^{2,4} pointed out the high sensitivity of λ_c to the geometrical parameters of the fibers. Because actual manufactured fibers may suffer from unavoidable geometrical imperfections, it is necessary to achieve a reliable measurement of λ_c . The technique prescribed in the normalized procedure for standard fibers, based on the measurement of higher-order modes' differential loss versus the fiber bending radius,⁵ is no longer valid for character-

izing MOFs because, due to the high NA of the fiber, higher-order modes are much less sensitive to bending than the corresponding modes in standard fibers. An alternative method based on the cutback technique was recently demonstrated to be suitable for MOFs.⁶ However, this differential technique may suffer dramatically from possible small changes of the launching conditions during the measurement. In this Letter, we report what is to our knowledge the first self-referenced nondestructive measurement of λ_c into MOFs. The method, based on azimuthal analysis of the far-field pattern at the output of the tested fiber, has already been successfully used for measurements in standard fibers.⁷ Because of an improved experimental setup (see Fig. 1), this method is applied for the first time to MOFs. A dual-wavelength (1064/532 nm) microchip pulsed Nd:YAG laser (repetition rate 5.4 kHz, pulse duration 0.6 ns) pumping a specially designed 4 m long MOF with an 800 nm zero dispersion provides a bright continuum (300–1700 nm) at the output that is used as the source for our measurement.⁸ The light from this fiber source (mean power 5 mW) is coupled by a slightly misaligned butt joint into the core of a 2 m sample of the fiber under test (FUT), providing the excitation of both the fundamental and the higher-order modes. The far-field pattern from the FUT output is scanned by means of a rotating bow-tie slit that is rotated at the frequency $f_s = 1.5$ Hz. The part of the light cross-

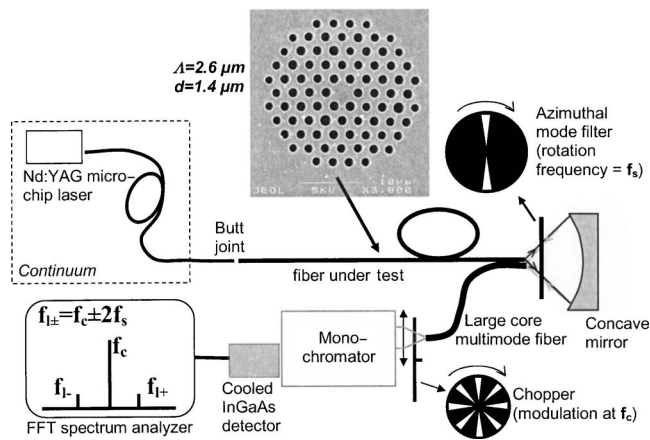


Fig. 1. Experimental setup. Inset, cross section of the microstructured fiber.

ing the slit is focused by a concave mirror onto the input face of a large-core-diameter multimode fiber. At the output of this collecting fiber, the signal is chopped at a frequency $f_c = 60$ Hz and spectrally filtered by a 0.5 nm spectral width monochromator. Finally, the optical power at the output of the monochromator is detected by an amplified thermoelectrically cooled InGaAs detector (EOS-IGA-020-TE2-H, detection area diameter 2 mm, response time 80 μ s), and the spectrum of the electric signal is displayed by a fast Fourier transform spectrum analyzer (FFT).

The power distribution of the fundamental mode propagating in MOFs has the same $\pi/3$ symmetry as that of the guiding structure cross section. As the azimuthal symmetry of each mode diffracted at the output is preserved by the Fourier transform, the far-field pattern from the fundamental mode also exhibits a $\pi/3$ symmetry. This gives rise to lateral lines at $f_c \pm 6f_s$ and to possible harmonics at $f_c \pm 6nf_s$ ($n \in \mathbb{N}$) in the spectrum of the detected signal at any wavelength. In the bimode regime, the symmetry of π of the first higher-order modes in fabricated MOFs generates new lateral lines at $f_l = f_c \pm 2f_s$, the amplitude of which depends on the part F of the output power carried by this mode ($0 \leq F \leq 1$). In the normalized measurement method (ITU-T G650) for conventional fibers, the criterion for determining λ_c corresponds to $F = 0.0225$ at the output of the FUT, assuming that the fundamental and the second modes are equally excited at the input.⁹ In the case of conventional fibers, it has already been demonstrated in Ref. 8 that $R(\lambda) = D(\lambda)$, in which

$$R(\lambda) = 10 \log (P_{11}/P_{01}) = 10 \log [F/(1 - F)],$$

$$D(\lambda) = 10 \log [2A_l/(A_c - 2A_l)]. \quad (1)$$

P_{11} and P_{01} are the power carried by the LP_{01} mode and the LP_{11} mode, respectively, and A_c and A_l are the linear amplitudes of the lines at f_c and f_l , respectively. Under these conditions, $D(\lambda_c) = -16.4$ dB for $F = 0.0225$. In the case of MOFs, because of the somewhat different spatial distribution of the power into the modes, $D(\lambda)$ becomes different from $R(\lambda)$, i.e., $D(\lambda_c) \neq -16.4$ dB. A large set of simulations that we

have carried out show that $D(\lambda_c)$ can vary in the range from approximately -22 to 14 dB according to the optogeometrical parameters of the considered MOF. Nevertheless, when crossing the cutoff wavelength, F increases from 0 to small but significant values and D suffers a very abrupt variation, allowing precise determination of λ_c . This method has been applied to a MOF manufactured by Alcatel using the standard stack and draw process. A scanning electron microscope picture representative of the characterized 2 m sample is shown in the inset of Fig. 1. Its average geometrical parameters, $\Lambda = 2.60 \pm 0.07$ μ m and $d = 1.43 \pm 0.04$ μ m ($d/\Lambda = 0.55$), have been evaluated by use of a commercial image analysis system. Figures 2(a) and 2(b) show typical spectra displayed by the spectrum analyzer in the single-mode domain ($D = -20$ dB) and in the bimode regime ($D = -8$ dB), respectively. As one can see in Fig. 2(a), unexpected lines rise at $f_c \pm 2f_s$ and $f_c \pm f_s$ in the single-mode domain. The lines at $f_c \pm 2f_s$ are essentially due to unavoidable alignment imperfections of the set fiber-azimuthal filter-mirror. Although they can be clearly identified, their level remains very low since it is only ~ 10 dB over the noise level and 46 dB below the reference line at f_c . The lines at $f_c \pm f_s$ are attributed to an additional slight unbalance in the rotation of the spatial filter. The effect of this rotation defect is more sensitive in the presence of the second mode because of the rapid radial variation of its intensity near the center [higher lines in the bi-

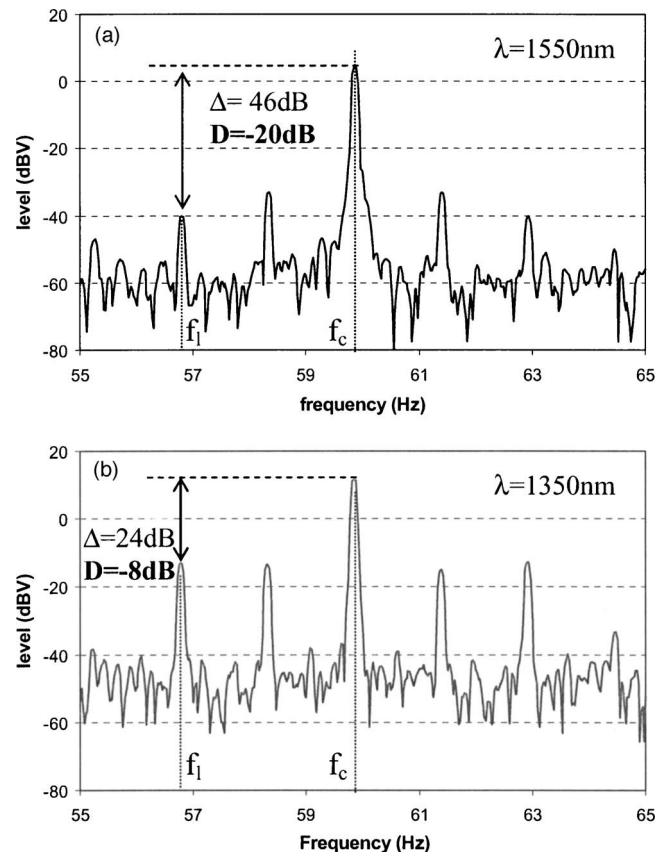


Fig. 2. Typical spectra measured with the setup described in Fig. 1(a) single-mode regime, (b) bimode regime [$\Delta = A_c(\text{dBV}) - A_l(\text{dBV})$].

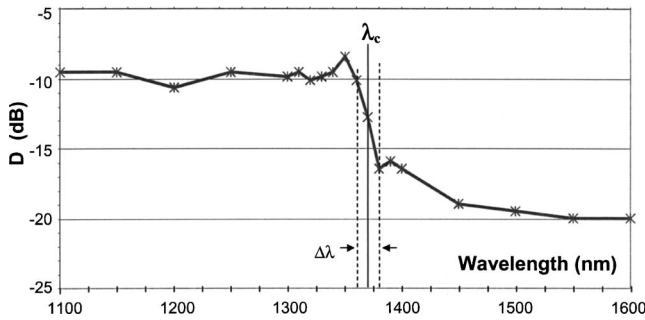


Fig. 3. Curve $D(\lambda)$ measured with the fiber shown in Fig. 1 and described in the text ($\lambda_c = 1370$ nm, $\Delta\lambda = 20$ nm).

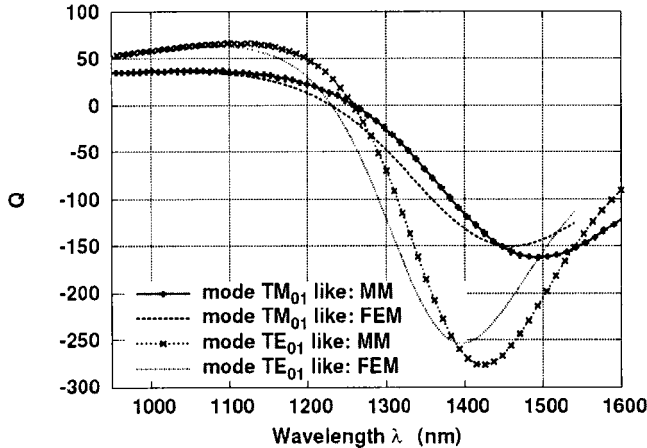


Fig. 4. Q as a function of wavelength for the first higher-order modes of the finite-size MOF described in the text. For clarity, the curves of the HE_{21} -like modes, close to those of the TE_{01} -like mode are not presented. The results from the finite-element method (FEM) and the multiple method (MM) are shown.

mode region as shown in Fig. 2(b)]. Let us note that the second mode may suffer discernible deformations (i.e., nonperfect π symmetry) in actual (nonideal) MOFs¹⁰ that are also likely to induce an increase of the lines at $f_c \pm f_s$.

The curve $D(\lambda)$, deduced from the lines at f_c and at f_l in the measured spectra, is shown in Fig. 3. It exhibits an abrupt 10 dB step when λ is decreased from 1380 to 1360 nm, allowing us to precisely locate λ_c at 1370 ± 10 nm. This result has been compared with the value of λ_c that has been theoretically determined for an ideal finite-size MOF ($\Lambda = 2.6$ μm and $d = 1.43$ μm) mimicking the fabricated one, as the wavelength $\lambda_{c\text{th}}$ for which the parameter $Q(\lambda) = \partial^2[\log \Im m(n_{\text{eff}})] / \partial[\log \lambda]^2$ exhibits a sharp minimum, n_{eff} being the complex effective index of the considered higher-order mode.² Two methods have been used to compute $n_{\text{eff}}(\lambda)$: a classical vectorial finite-element method with perfect matched layers at the outer boundaries of the modeled structure,¹¹ and the well-established multipole method.¹² On the curves of $Q(\lambda)$ shown in Fig. 4, we can notice an ~ 15 nm difference between $\lambda_{c\text{th}}$ obtained by the two methods for each of the four EM higher-order modes [TE₀₁-like, TM₀₁-like, a degenerate pair HE_{21(x,y)}-like]. This discrepancy is attributed to the influence

of the perfectly matched layer in the finite-element method; no such technique is needed with the multiple method. However, the two methods provide similar results. $\lambda_{c\text{th}}$ of the TM₀₁-like mode is found to be about 85 nm higher than that of the HE₂₁-like mode and 70 nm higher than that of the TE₀₁-like mode. The theoretical cutoff region for these higher-order modes extends from 1.39 to 1.49 μm . This result is close but slightly higher than the experimental one, as was also noted in Ref. 6. This is not surprising if we consider the following three points. First, the simulations address only the confinement loss of the ideal MOF and do not take into account the effects of the geometrical imperfections of the actual fiber. Second, the criterion used for the experimental determination of λ_c is different from the one used in the simulations, and the two cannot be directly related. Finally, it is worth noting that we do not control the polarization of the light launched into the FUT. This means that we do not control the part of the propagating power that is carried by each higher-order mode. The fact that their cutoff wavelengths are distributed over about 100 nm could explain the irregular shape and the slow decrease of the curve $D(\lambda)$ between 1390 and 1500 nm.

In conclusion, we have proposed a new efficient self-referenced method for accurately measuring the cutoff wavelength of MOFs. The first reported measurements are in fairly good agreement with the theoretical predictions. Furthermore, this method makes it possible to study the length and the curvature dependence of λ_c in MOFs.

We are grateful to our colleagues Vincent Couderc *et al.* from Xlim for providing us with a prototype of the continuum source they have developed. L. Labonté's e-mail address is labonte@xlim.fr.

References

1. P. St. J. Russell, *Science* **299**, 358 (2003).
2. B. T. Kuhlmey, R. C. McPhedran, and C. Martijn de Sterke, *Opt. Lett.* **27**, 1684 (2002).
3. K. Ranka, R. S. Windeler, and A. J. Stentz, *Opt. Lett.* **25**, 25 (2000).
4. G. Renversez, F. Bordas, and B. Kuhlmey, *Opt. Lett.* **30**, 1264 (2005).
5. CEI/IEC International Standard 793-1-C7A, "Cutoff wavelength measurement for single-mode fibre."
6. J. R. Folkenberg, N. A. Mortensen, K. P. Hansen, T. P. Hansen, H. R. Simonsen, and C. Jakobsen, *Opt. Lett.* **28**, 1882 (2003).
7. J. M. Blondy, A. M. Blanc, M. Clapeau, and P. Facq, *Electron. Lett.* **23**, 522 (1987).
8. P. Champert, V. Couderc, P. Leproux, S. Février, V. Tombelaine, L. Labonté, P. Roy, C. Froehly, and P. Nérin, *Opt. Express* **12**, 4366 (2004).
9. D. Pagnoux, J. M. Blondy, P. DiBin, P. Faugeras, and P. Facq, *J. Lightwave Technol.* **12**, 385 (1994).
10. N. A. Mortensen, M. D. Nielsen, J. R. Folkenberg, K. P. Hansen, and J. Laegsgaard, *J. Opt. A* **6**, 221 (2004).
11. D. Ferrarini, L. Vincenti, M. Zoboli, A. Cucinotta, and S. Selleri, *Opt. Express* **10**, 1314 (2002).
12. B. Kuhlmey, T. P. White, G. Renversez, D. Maystre, L. C. Botten, C. Martijn de Sterke, and R. C. McPhedran, *J. Opt. Soc. Am. B* **10**, 2331 (2002).